Temperature dependence of the interband critical-point parameters of InP

P. Lautenschlager, M. Garriga, and M. Cardona
Max-Planck-Institut für Festkörperforschung, Heisenbergstrasse 1, D-7000 Stuttgart 80, Federal Republic of Germany
(Received 21 April 1987)

Spectroscopic ellipsometry has been used to measure the dielectric function $\epsilon(\omega)$ of InP from 30 to 750 K in the 1.3–5.5-eV photon-energy region. By performing a line-shape analysis of the structures observed, the temperature dependence of the interband critical-point parameters (strength, threshold energy, broadening, and excitonic phase angle) has been determined. The decrease in energy and the increase in broadening with increasing temperature are analyzed in terms of averaged frequencies of phonons giving rise to the renormalization of the band states due to electron-phonon interaction.

I. INTRODUCTION

InP has become an important material for optoelectronic devices. It is used as substrate for the quarternary compound $In_{1-x}Ga_xAs_yP_{1-y}$, whose band gap can be tuned between 0.75 and 1.35 eV at room temperature, when grown lattice matched to the InP substrate.[1]

A basic quantity describing the linear response of the material to the electric field of an electromagnetic wave is the dielectric function $\epsilon(\omega)$. This function, on the other hand, is directly related to the electronic band structure and thus allows experimental investigations of the effects on the band structure of changes in the material parameters and of external perturbations. Spectroscopic ellipsometry is highly suitable to determine the dielectric function of many semiconductors in the 1.5–6-eV region[2] and to investigate the dependence of the dielectric function on perturbations such as temperature,[3–8] concentration of donors and acceptors,[9,10] and composition in mixed crystals.[11–14] The structures observed in the $\epsilon(\omega)$ spectra are attributed to interband critical points (CP's) which can be analyzed in terms of standard analytic line shapes:[15,16]

$$\epsilon(\omega)=C-Ae^{i\phi}(\omega-E+i\Gamma)^n \ . \tag{1}$$

The critical-point parameters amplitude A, energy threshold E, broadening Γ, and excitonic phase angle ϕ are determined by fitting the numerically obtained second-derivative spectra $d^2\epsilon(\omega)/d\omega^2$ of the experimental $\epsilon(\omega)$. (The exponent n has the value $-\frac{1}{2}$ for one-dimensional (1D), 0 [logarithmic, i.e., $\ln(\omega-E+i\Gamma)$] for 2D, and $\frac{1}{2}$ for 3D CP's. Discrete excitons with Lorentzian line shape are represented by $n=-1$.) The CP's are directly related to regions of large or singular joint electronic density of states, so that direct information on the energy separation and broadening of valence and conduction bands is obtained which can be compared to band-structure calculations.

The band structure of InP, as calculated by Chelikowsky and Cohen,[17] is shown in Fig. 1. Several interband transitions related to CP's at different parts of the Brillouin zone (BZ) are indicated. In order to determine the energies of interband CP's in InP, ellipsometric measurements[11,18] have been performed. Other optical techniques such as luminescence[19–21] (for the E_0 transition), absorption,[22] resonant Raman scattering,[23] reflectance,[24–27] thermoreflectance,[28] electroreflectance,[29–35] wavelength-modulated reflectance,[36,37] and wavelength-modulated photovoltaic effect[38] have also been used. Concerning the temperature dependence of the critical-point parameters, only very few experimental data are available. The dependence on temperature has been measured by absorption for the E_0 transition of InP (Ref. 22) and for the E_1 CP by reflectance,[24] in both cases only up to 300 K.

For a theoretical investigation of the energy shift of CP's the thermal expansion as well as the electron-phonon interaction must be taken into account. Microscopic calculations of the electron-phonon interaction, including the full band structure and phonon dispersion, have been presented recently for GaAs, another III-V compound.[39] These calculations were able to describe the observed dependence of the broadening of CP's on temperature. The dependence of CP parameters on temperature for some other zinc-blende-type III-V compounds [(InSb (Ref. 4) and GaAs (Ref. 8)] has already been reported.

In this paper we investigate the temperature depen-

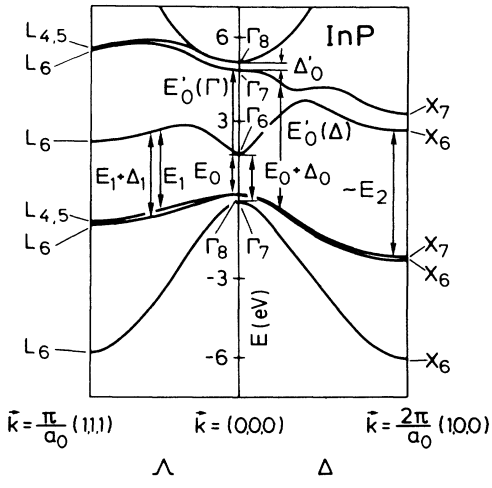

FIG. 1. Band structure of InP calculated by Chelikowsky and Cohen (Ref. 17) with nonlocal pseudopotentials.

dence of the optical constants and the CP parameters of undoped InP from 30 to 750 K in the photon-energy range from 1.3 to 5.6 eV, as measured by spectroscopic ellipsometry. We present data for the E_0, $E_0+\Delta_0$, E_1, and $E_1+\Delta_1$ transitions, and for the transitions in the uv region, mainly E_0' and $E_0'+\Delta_0'$. In Sec. II we describe the experimental procedure, in Sec. III we present the measured temperature dependence of the CP parameters. These results are discussed in Sec. IV.

II. EXPERIMENTAL

The measurements were carried out on an n-type InP sample, grown by the Czochralski method. The sample was compensated, with $n=N_D-N_A=5\times10^{15}$ cm^{-3} (at 300 K) and had a (111) surface orientation. The procedure of etching the sample and mounting into the cryostat has been described in Ref. 8. Details of the automatic spectral ellipsometer with rotating analyzer are also described elsewhere.[3,40]

The energy mesh of the experimental points was 10 meV in the 1.7–5.6-eV photon energy region while in the region of the edge exciton (1.3–1.6 eV) a 2-meV mesh was used, the spectral slit width being better than 1 meV. All spectra were taken at an angle of incidence of 67.5°.

III. RESULTS

The quantity measured by ellipsometry is the complex reflectance ratio ρ, defined as $\rho=r_p/r_s$, where r_p and r_s are the amplitude reflection coefficients parallel and perpendicular to the plane of incidence, respectively. If the two-phase model[41] (ambient-medium–crystal) is valid the dielectric function $\epsilon(\omega)=\epsilon_1(\omega)+i\epsilon_2(\omega)$ of an isotropic material can be directly calculated from the measured ρ. In our case, however, due to the transfer of the sample to the cryostat and the process of outgassing, an oxide layer was present. By assuming the three-phase model[41] for the sample and that the oxide layer has the same dielectric function as the oxide on GaAs (Ref. 42) we find that a thickness of $d=12.3$ Å gives at room temperature good agreement with data from the literature.[2] Figure 2 shows the comparison of our data from the three-phase model with those obtained directly after wet-chemical processing techniques.[2]

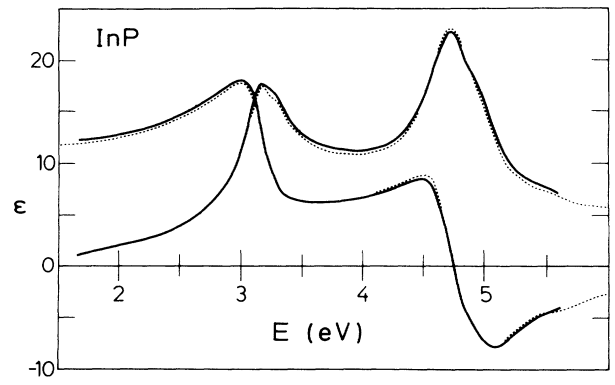

FIG. 2. Solid line: real (ϵ_1) and imaginary (ϵ_2) part of the dielectric function of InP measured at room temperature with the sample inside our cryostat. Data are corrected for a 12.3-Å layer of GaAs oxide. Dashed line: data from Ref. 2, obtained directly after wet-chemical processing (without mounting in cryostat).

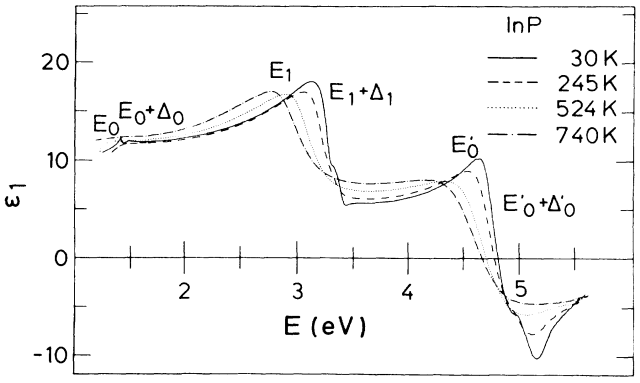

FIG. 3. Real part of the dielectric function of InP for several temperatures.

In Figs. 3 and 4 we present the spectra obtained for the real and imaginary parts of the dielectric function of InP for several temperatures after a correction for 12.3 Å of GaAs oxide. The structures, corresponding to the E_1, $E_1+\Delta_1$, and E_0' transitions, are clearly resolved. At low temperatures small structures due to the E_0, $E_0+\Delta_0$, and $E_0'+\Delta_0'$ are also visible.

For the line-shape analysis and in order to obtain the critical-point parameters, the second-derivative spectra, $d^2\epsilon/d\omega^2$, of the complex dielectric function were calculated numerically.[43] Figure 5 shows the numerical second-derivative spectrum of ϵ_1 at 30 K in the spectral regions where structures are observed. The lines represent the best fits to standard critical-point line shapes, derived from Eq. (1):

$$\frac{d^2\epsilon}{d\omega^2}=-n(n-1)Ae^{i\phi}(\omega-E+i\Gamma)^{n-2},\quad n\neq0$$
$$\frac{d^2\epsilon}{d\omega^2}=Ae^{i\phi}(\omega-E+i\Gamma)^{-2},\quad n=0\ . \tag{2}$$

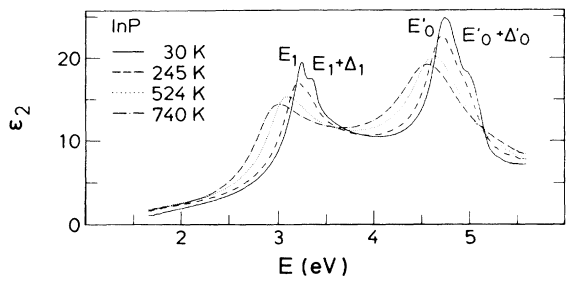

FIG. 4. Imaginary part of the dielectric function of InP for several temperatures.

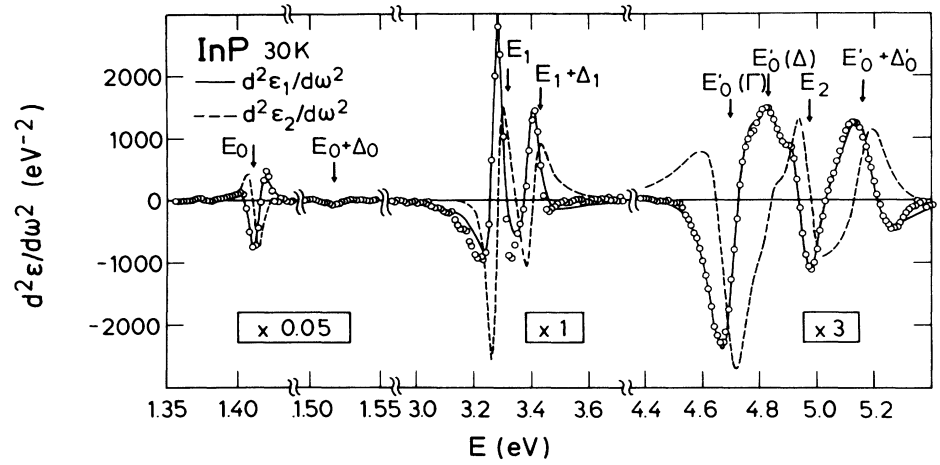

FIG. 5. Fits to the second derivatives of the real (solid line) and imaginary (dashed line) parts of the dielectric function of InP measured as a function of energy at 30 K. The readings from the vertical scale have to be divided by the factor given in the box under the various structures. Note the change in the energy scale for the E_0 and $E_0+\Delta_0$ transitions.

The fit was performed simultaneously for the real and imaginary part of $d^2\epsilon/d\omega^2$, using a least-squares procedure. The exponent n has the value $-\frac{1}{2}$ for one-dimensional (1D), 0 [logarithmic i.e., $\ln(\omega-E+i\Gamma)$] for 2D, and $\frac{1}{2}$, for 3D CP's. If the angle ϕ in the phase factor $e^{i\phi}$ takes values which are integer multiples of $\pi/2$, the line shape corresponds to transitions between uncorrelated one-electron bands while noninteger multiples represent the inclusion of excitonic effects by allowing a mixture of two CP's.[8,15,44,45]

The E_0 and $E_0+\Delta_0$ structures are fitted with excitonic line shapes [$n=-1$ in Eq. (2)] only in the real part of the dielectric function and up to 80 K. At higher temperatures the structures become too weak and too broad to perform a line-shape analysis, so that the energies are simply determined from the maxima in the $\epsilon_1(\omega)$ spectra [the peak in $\epsilon_1(\omega)$ are rather symmetric at these temperatures, a fact which justifies this definition]. The E_1 and $E_1+\Delta_1$ CP's are fitted with a 2D line shape, both with the same phase angle ϕ and a constant spin-orbit splitting $\Delta_1=136$ meV, determined from the low-temperature spectra. In addition, the broadening Γ of both CP's is assumed to be the same for each temperature. The other structures shown in Fig. 5 are analyzed with 2D CP line shapes.

The energies for the various CP's as a function of temperature are shown in Fig. 6. The energies of the $E_1+\Delta_1$ CP are not shown. They simply run parallel to those of E_1, shifted by 136 meV. The solid lines represent the fit of the data with an equation containing the Bose-Einstein occupation factor for phonons:[3,46]

$$E(T)=E_B-a_B\left[1+\frac{2}{e^{\Theta/T}-1}\right]. \tag{3}$$

Besides the changes of the band structure by thermal expansion of the lattice, the temperature dependence is mainly due to electron-phonon interaction. The parameter Θ describes a mean frequency of the phonons involved, a_B the strength of the interaction.[46]

The temperature dependence of the $E_0'+\Delta_0'$ structure has been described by the linear equation

$$E(T)=E_L-\lambda T\ . \tag{4}$$

The values of the parameters E_B, a_B, Θ as well as E_L, λ are listed in Table I, together with the 95% confidence limits.

TABLE I. Parameters involved in the temperature dependence of the critical-point energies in InP. Values of the parameters E_B, a_B, and Θ from the fit with $E(T)=E_B-a_B[1+2/(e^{\Theta/T}-1)]$ and with $E(T)=E_L-\lambda T$ (for $E_0'+\Delta_0'$). The 95% confidence limit is given in parentheses.

InP	E_L (eV)	λ (10^{-4} eV K^{-1})	E_B (eV)	a_B (meV)	Θ (K)	Line shape
E_0			1.629(111)	217(113)	697(177)	from maximum in ϵ_1 (up to 430 K)
$E_0+\Delta_0$			1.579(36)	61(38)	370(158)	from maximum in ϵ_1 (up to 430 K)
E_1			3.348(7)	68(10)	224(30)	2D
E_0'			4.867(42)	163(44)	775(127)	2D
$E_0'+\Delta_0'$	5.112(13)	4.25(45)				2D (up to 500 K)

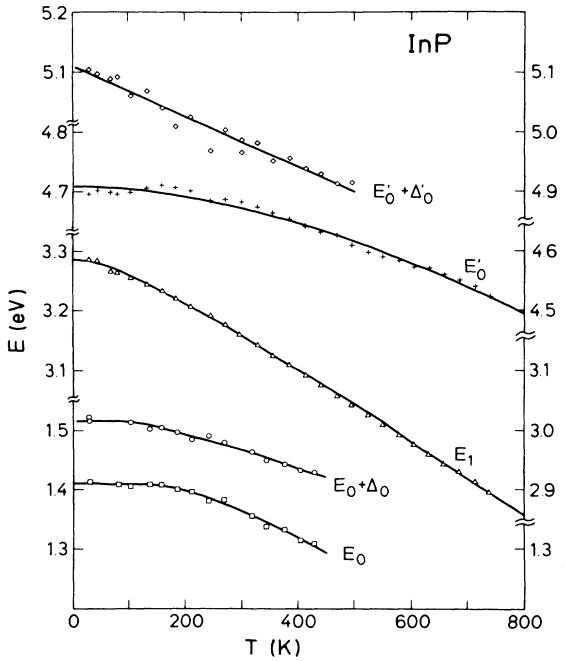

FIG. 6. Temperature dependence of the interband critical-point energies of InP. The solid lines represent the best fits with Eq. (3). Typical error bars for the experimental points are given in Table III, the fit parameters in Table I.

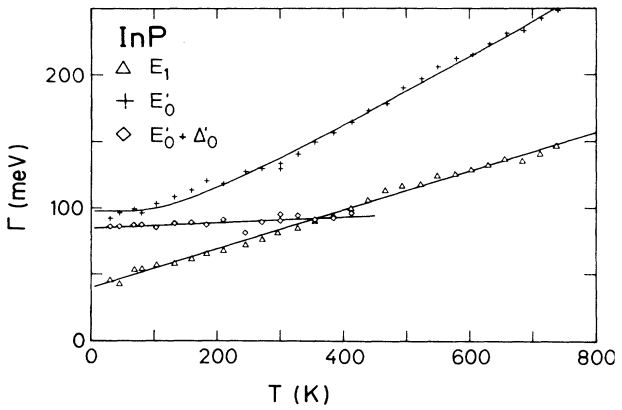

FIG. 7. Temperature dependence of the broadening parameters of the critical points. The solid lines represent fits to Eq. (5) or (6). The function used and the corresponding fit parameters are given in Table II.

The temperature dependence of the broadening parameters of the E_1, E_0', and $E_0'+\Delta_0'$ transitions are shown in Fig. 7. We remind the reader that the broadening of the $E_1+\Delta_1$ CP has been chosen to be the same as that for E_1. Fits to the broadenings as a function of temperature are performed with the equation

$$\Gamma(T)=\Gamma_0\left[1+\frac{2}{e^{\Theta/T}-1}\right]+\Gamma_1 \tag{5}$$

for the E_0' transition and with

$$\Gamma(T)=\Gamma_L+\gamma T \tag{6}$$

for the E_1 and the $E_0'+\Delta_0'$ CP's.

The resulting parameters are given in Table II with the 95% confidence limits.

The temperature dependence of the other two parameters, describing a CP line shape according to Eq. (1) or (2), the phase angle ϕ and the amplitude A, are shown in Figs. 8 and 9.

IV. DISCUSSION

A. E_0 and $E_0+\Delta_0$ transitions

In InP, E_0 and $E_0+\Delta_0$ represent the lowest direct gaps and are localized at the Γ point of the BZ. The strength of these transitions is very low, they appear only as a small peak in the real part of the dielectric function (Fig. 3). Because of the inherent poor accuracy of rotating-analyzer ellipsometers for small ϵ_2 (Refs. 2 and 47) the increase of the absorption at the lowest band edge cannot be observed. From the maxima in the real part of the dielectric function the energies of the E_0 and $E_0+\Delta_0$ transitions could be determined up to 420 K. In Table III the energies of interband transitions are listed for several temperatures as measured by various techniques, including the results of the present work. Linear temperature coefficients for the CP's are often given in the literature. Table IV shows a comparison with our ellipsometric data.

B. E_1 and $E_1+\Delta_1$ transitions

The E_1 and $E_1+\Delta_1$ transitions take place along the Λ directions of the BZ (see Fig. 1). Their line shape is best

TABLE II. Parameters involved in the temperature dependence of the broadenings of critical points in InP. Values of the parameters Γ_0, Γ_1, and Θ from the fit with $\Gamma(T)=\Gamma_0[1+2/(e^{\Theta/T}-1)]$ or $\Gamma(T)=\Gamma_L+\gamma T$. All CP's listed have been fitted with a 2D line shape.

InP	Γ_1 (meV)	Γ_0 (meV)	Θ (K)	Γ_L (meV)	γ (10^{-4} eV K^{-1})	Temperature range (K)
E_1				39.7(2.1)	1.46(5)	30–750
E_0'	45(12)	52(14)	384(83)			30–750
$E_0'+\Delta_0'$				84(3)	0.22(12)	30–420

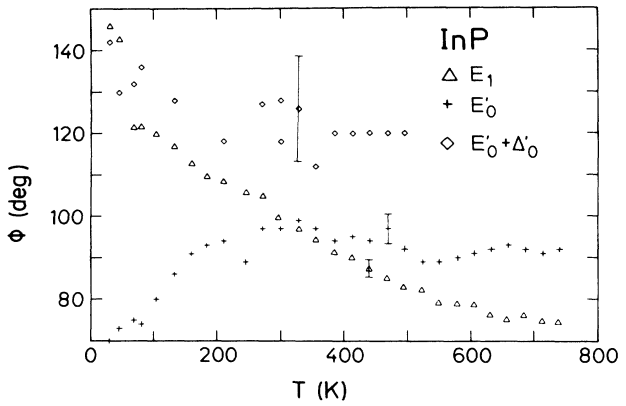

FIG. 8. Temperature dependence of the phase angle ϕ defined in Eq. (2) for the interband transitions in InP.

represented by a 2D CP over the whole temperature range, although the excitonic phase angle ϕ at low temperatures has a large value of about 140° and decreases to $\phi=100°\pm3°$ at room temperature. As already pointed out in Ref. 8, on the basis of the theory of the contact exciton[15,48,49] Eq. (1) or (2) should represent CP line shapes only for small values of ϕ. Kelso *et al.*[11] have also found $\phi=106°\pm4°$ from a fit to a 2D line shape at room temperature. Because of the restriction of the contact interaction to $\phi \ll 90°$ they suggested a 3D CP, which corresponds to $\phi=57°\pm5°$. The deviation of theoretical and experimental line shapes, however, was larger for a 3D M_1 CP than for a 2D M_0 CP.[11] The temperature dependent measurements reported here show that the 2D model yields a better description of the data over the whole temperature range.

The fit is performed with the same phase angle ϕ for the E_1 and $E_1+\Delta_1$ CP's with a constant $\Delta_1=136$ meV. In addition, the broadening of the two CP's is assumed to be the same. The broadening of an electronic state is roughly proportional to the electronic density of states at its energy.[46] Thus the broadening of $E_1+\Delta_1$ should

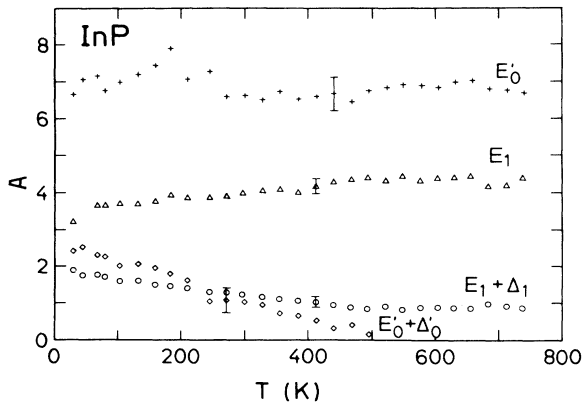

FIG. 9. Temperature dependence of the amplitudes of the critical points, defined in Eq. (2), for InP.

be at least as large as for E_1 since for the lower split-off valence band there is a larger electronic density of states than for the upper one. For fits with Γ_{E_1} and $\Gamma_{E_1+\Delta_1}$ as free parameters, we obtained above 150 K somewhat smaller values for $\Gamma_{E_1+\Delta_1}$ than for Γ_{E_1}. This is probably an artifact of the fit procedure, because Γ becomes comparable with the energy separation between the structures Δ_1. Thus we set $\Gamma_{E_1}=\Gamma_{E_1+\Delta_1}$ and find no significant worsening of the quality of the fit. In Table III, a comparison of CP energies with values from the literature is given.

The amplitudes for the E_1 and $E_1+\Delta_1$ transitions can be estimated within the one-electron approximation by[50,51]

$$A_{E_1} \cong \frac{44(E_1+\Delta_1/3)}{a_0 E_1^2}=2.4\ ,$$
$$A_{E_1+\Delta_1} \cong \frac{44(E_1+2\Delta_1/3)}{a_0(E_1+\Delta_1)^2}=2.2\ , \tag{7}$$

where the lattice constant a_0 is in Å and the energies E_1 and $E_1+\Delta_1$, taken at 300 K, are in eV. By taking into account a correction for the terms linear in $\mathbf{k}$ for $\mathbf{k}$ perpendicular to $\langle 111 \rangle$ (Refs. 52–54) and assuming the averaged matrix element Π of $\mathbf{p}$ to be equal to that for Si ($\Pi \sim 0.1$ bohr^{-1}, Ref. 52), we get $A_{E_1}=2.8$ and $A_{E_1+\Delta_1}=2.0$. Experimentally, $A_{E_1}=4.0$ and $A_{E_1+\Delta_1}=1.25$ have been found at room temperature. The value of $A_{E_1+\Delta_1}/A_{E_1}=0.31$ at room temperature is, however, in good agreement with $A_{E_1+\Delta_1}/A_{E_1}=0.36$ from other ellipsometric measurements.[18] However, the ratio $A_{E_1+\Delta_1}/A_{E_1}$ decreases slightly with increasing temperature, as seen from Fig. 9. This decrease is possibly an artifact of the fit arising from the worsening resolution of these structures with increasing temperature.

C. E'_0 and E_2 transitions

From the band-structure calculations of Chelikowsky and Cohen[17] four CP's are expected in the 4.5–5.6-eV energy region. Two of them correspond to transitions at the Γ point from the highest valence band to the second lowest conduction band: $\Gamma_8^v \rightarrow \Gamma_7^c$ (at 4.64 eV) and $\Gamma_8^v \rightarrow \Gamma_8^c$ (at 5.13 eV, see Fig. 1). They are labeled $E'_0(\Gamma)$ (4.695 eV) and $E'_0+\Delta'_0$ (5.166 eV) in Fig. 5. A further transition, found in the calculations[17] for $(2\pi/a_0)(0.2,0,0)$ for 4.80 eV, is labeled $E'_0(\Delta)$ (4.836 eV) in Fig. 5. The E_2 transitions taking place at an interband plateau near $(2\pi/a_0)(0.75,0.25,0.25)$ are expected at 5.0 eV.[17] The structure at 4.961 eV in Fig. 5 is assigned to these E_2 transitions. At high temperatures only the structures labeled E'_0 and $E'_0+\Delta'_0$ can be resolved. In earlier electroreflectance measurements the $E'_0+\Delta'_0$ CP has been attributed to E_2 transitions.[31] However, following theoretical considerations about the spin-orbit splitting of the conduction band, Δ'_0, the structure has more recently been assigned to $E'_0+\Delta'_0$ transitions.[11]

In ionic materials the electronic states at the Γ point have predominant cation or anion character. Thus the valence-band splitting Δ_0 in zinc-blende-type materials is

mainly determined by the atomic spin-orbit splitting of the anion, the conduction-band splitting Δ_0' mainly by that of the cation.[55] Because of its atomic origin the spin-orbit splitting should be independent of temperature. The temperature dependence of E_0' and $E_0'+\Delta_0'$, shown in Fig. 6, however, indicates that this is not the case. The value of $\Delta_0'=0.31$ eV calculated by Chadi[55] is only found experimentally at room temperature (see also Table III). On this basis the assignment of the structure at higher energies to $E_0'+\Delta_0'$ transitions, as suggested in Ref. 11, instead of the E_2 CP's may be questioned. Also, the clearly different phase angles of both CP's, displayed in Fig. 8,

TABLE III. Energies of critical points in InP at several temperatures. All values are in eV.

Temperature (K)	E_0	$E_0+\Delta_0$	E_1	$E_1+\Delta_1$	E_0' range	E_2 range
			Experiment			
2	1.4241[a]					
	1.4182[b]					
	1.4183[c]					
	1.4185[c]					
	1.4185[d]					
4.2	1.423[e]	1.531[e]				
5	1.4182[f]	1.5263[f]	3.24[p]	3.38[p]	4.78[p]	5.10[p], 5.77[p]
6	1.4205[g]					
20	1.4205[g]					
30	1.414(1)[h]	1.522(5)[h]	3.287(2)[h]	3.423(2)[h]	4.695(4)[h] 4.836(3)[h] 5.166(9)[h]	4.961(5)[h]
77	1.4135[g]					
80	1.413[i]	1.525[i]	3.25[u]	3.37[u]	4.70[u] 4.78[u]	4.99[u]
	$\Delta_0=0.10$[r]		$\Delta_1=0.13$[r]		4.8[r]	5.05[r]
82	1.403(4)[h]	1.520(8)[h]	3.266(2)[h]	3.402(2)[h]	4.696(5)[h] 5.093(13)[h]	
100		1.509[t]				
296	1.26[j]		3.15[j]	3.29[j]		5.0[j]
	1.3511[g]					
	1.34[k]	1.45[k]	3.12[k] 3.19[k]	3.27[k] 3.34[k]	4.72[k] 4.79[k]	5.04[k], 5.24[k], 5.6[k]
						5.02[x], 5.25[x] 5.6[x]
	1.351[j]	1.446[j]				
	1.345[l]	1.465[l]	3.130[l]	3.270[l]		
296	1.337[m]	1.449[m]	3.122[m] 3.158[v]	3.256[m] 3.291[v]	4.67[v], 4.79[v]	
	1.349[n]	1.472[n]	3.181[n]	3.326[n]		
	1.345[o]	1.469[o]	3.1584[w]	3.2896[w]		
	$\Delta_0=0.11$[s]		$\Delta_1=0.16$[s]			
	1.357(8)[h]	1.465(12)[h]	3.162(2)[h]	3.298(2)[h]	4.688(5)[h], 4.985(14)[h]	
683			2.931(3)[h]	3.067(3)[h]	4.552(10)[h]	
			Theory			
	1.5[p]		3.2[p]	3.22[p]	4.88[p], 5.5[p]	4.7[p], 4.71[p] 5.02[p], 5.77[p]
	1.50[q]	1.71[q]	3.13[q]	3.28[q]	4.64[q], 4.8[q], 5.13[q]	5.0[q], 5.62[q]

[a]Reference 20. [b]Reference 19. [c]Reference 26. [d]Reference 21. [e]Reference 38. [f]Reference 29. [g]Reference 22. [h]Present work.
[i]Reference 27. [j]Reference 24. [k]Reference 31. Two structures for each E_1 and $E_1+\Delta_1$. [l]Reference 32. [m]Reference 33. [n]Reference 34. [o]Reference 35. [p]Reference 36.
[q]Reference 17. [r]Reference 28. [s]Reference 30. [t]Reference 23. [u]Reference 37. [v]Reference 11. [w]Reference 18. [x]Reference 25.

TABLE IV. Linear temperature coefficients of the energies of the critical points in InP. All values are in 10^{-4} eV K.

$-dE_0/dT$	$-d(E_0+\Delta_0)/dT$	$-dE_1/dT$	$-dE_0'/dT$	$-d(E_0'+\Delta_0')/dT$
		Experiment		
		Between 200 and 300 K		
2.9[a]		4.2[c]		
3.3(5)[b]	2.7(5)[b]	5.6(1)[b]	1.9(3)[b]	4.3(5)[b]
		Between 600 and 800 K		
		6.0(2)[b]	3.2(4)[b]	
		Theory		
		Between 200 and 300 K		
		3.6[d]		3.2[d,e]

[a]Reference 22.
[b]Present work.
[c]Reference 24.
[d]Y. F. Tsang, B. Gong, S. S. Mitra, and J. F. Vetelino, Phys. Rev. B **6**, 2330 (1972).
[e]For E_2 band gap.

are against the assumption of both CP's being localized around Γ. On the other hand, the calculations by Chelikowsky and Cohen[17] support the assignment. We retain this assignment, i.e., the two main structures between 4 and 5.5 eV are assumed to correspond to E_0' and $E_0'+\Delta_0'$ transitions near the Γ point of the BZ (see Figs. 1 and 5). We should keep, however, in mind that the peculiar temperature dependence of Δ_0' shown in Fig. 6 must be due to contributions of other transitions to these structures.

The temperature dependence of the E_0' CP is described by the Bose-Einstein function [Eq. (3)], whereas the CP energy of the weaker $E_0'+\Delta_0'$ CP, which can be resolved only up to 500 K, shows linear behavior with temperature (Fig. 6). The energies of the E_0' CP are around 200 K slightly higher than at lower temperatures. Besides, the mean phonon frequency Θ, obtained from the fit to Eq. (3), has an unexpected high value of 775 K (the highest frequency of phonons in InP corresponds to 496 K). This fact may be due to the complicated structure of the E_0' transitions and the multitude of possible CP's in this spectral region which may give rise to an averaging over several CP's.

The temperature dependence of the broadenings of the E_0' transitions can be described with an averaged phonon temperature of 384 K (see Table II), while the broadenings of the $E_0'+\Delta_0'$ CP are found to be nearly temperature independent (see Fig. 7).

V. CONCLUSION

We have measured the temperature dependence of the dielectric function of InP by means of spectroscopic ellipsometry in the 1.3–5.6-eV photon energy region between 30 and 750 K. From a line shape analysis we have obtained the temperature dependence of the interband critical-point parameters (energy, broadening, amplitude, excitonic phase angle) of the E_1, E_0', and $E_0'+\Delta_0'$ transitions. Also, the dependence of the energy of the E_0 and $E_0+\Delta_0$ transitions on temperature has been determined.

ACKNOWLEDGMENTS

One of us (M.G.) acknowledges financial support of the Caixa de Pensions "la Caixa," Barcelona (Spain). We would like to thank Dr. G. Müller (Universität Erlangen) for supplying the InP. We also thank W. Neu for help with the cryostat, G. Kisela and co-workers at the Max-Planck-Institute for sample preparation, and M. Bleder and A. Birkner for help with the construction of the ellipsometer. In addition, we thank H. Hirt, M. Siemers, and P. Wurster for expert technical help.

[1]E.g., H. C. Casey and M. B. Panish, *Heterostructure Lasers* (Academic, New York, 1978).
[2]D. E. Aspnes and A. A. Studna, Phys. Rev. B **27**, 985 (1983).
[3]L. Viña, S. Logothetidis, and M. Cardona, Phys. Rev. B **30**, 1979 (1984).
[4]S. Logothetidis, L. Viña, and M. Cardona, Phys. Rev. B **31**, 947 (1985).
[5]L. Viña, H. Höchst, and M. Cardona, Phys. Rev. B **31**, 985 (1985).
[6]S. Logothetidis, P. Lautenschlager, and M. Cardona, Phys. Rev. B **33**, 1110 (1986).
[7]S. Logothetidis, M. Cardona, P. Lautenschlager, and M. Garriga, Phys. Rev. B **34**, 2458 (1986).
[8]P. Lautenschlager, M. Garriga, S. Logothetidis, and M. Cardona, Phys. Rev. B **35**, 9174 (1987).
[9]L. Viña and M. Cardona, Phys. Rev. B **29**, 6739 (1984).
[10]L. Viña and M. Cardona, Phys. Rev. B **34**, 2586 (1986).
[11]S. M. Kelso, D. E. Aspnes, M. A. Pollack, and R. E. Nahory, Phys. Rev. B **26**, 6669 (1982).
[12]L. Viña, C. Umbach, M. Cardona, and L. Vodopyanov, Phys. Rev. B **29**, 6752 (1984).
[13]P. Lautenschlager, S. Logothetidis, L. Viña, and M. Cardona, Phys. Rev. B **32**, 3811 (1985).
[14]D. E. Aspnes, S. M. Kelso, R. A. Logan, and R. Bhat, J.

Appl. Phys. **60**, 754 (1986).
[15]M. Cardona, *Modulation Spectroscopy,* Suppl. 11 of *Solid State Physics,* edited by F. Seitz, D. Turnbull, and H. Ehrenreich (Academic, New York, 1969).
[16]D. E. Aspnes, in *Handbook on Semiconductors,* edited by M. Balkanski (North-Holland, Amsterdam, 1980), Vol. 2, p. 109.
[17]J. R. Chelikowsky and M. L. Cohen, Phys. Rev. B **14**, 556 (1976).
[18]M. Erman, J. P. Andre, and J. LeBris, J. Appl. Phys. **59**, 2019 (1986).
[19]A. M. White, P. J. Dean, L. L. Taylor, R. C. Clarke, D. J. Ashen, and J. B. Mullin, J. Phys. C **5**, 1727 (1972).
[20]J. U. Fischbach, G. Benz, N. Stahl, M. H. Pilkuhn, and K. W. Benz, Solid State Commun. **11**, 721 (1972).
[21]W. Rühle and W. Klingenstein, Phys. Rev. B **18**, 7011 (1978).
[22]W. J. Turner, W. E. Reese, and G. D. Pettit, Phys. Rev. **136**, A1467 (1964).
[23]W. Kauschke and M. Cardona, Phys. Rev. B **33**, 5473 (1986).
[24]M. Cardona, J. Appl. Phys. Suppl. **32**, 2151 (1961).
[25]S. S. Vishnubhatla and J. C. Woolley, Can. J. Phys. **46**, 1769 (1968).
[26]F. Evangelisti, J. U. Fishbach, and A. Frova, Phys. Rev. B **9**, 1516 (1974).
[27]V. V. Sobolev, V. I. Donetskikh, and E. F. Zagainov, Fiz. Tekh. Polyprovodn. **12**, 1089 (1978) [Sov. Phys.—Semicond. **12**, 646 (1978)].
[28]E. Matatagui, A. G. Thompson, and M. Cardona, Phys. Rev. **176**, 950 (1968).
[29]J. Camassel, P. Merle, L. Bayo, and H. Mathieu, Phys. Rev. B **22**, 2020 (1980).
[30]K. L. Shaklee, M. Cardona, and F. H. Pollak, Phys. Rev. Lett. **16**, 48 (1966).
[31]M. Cardona, K. L. Shaklee, and F. H. Pollak, Phys. Rev. **154**, 696 (1967).
[32]E. H. Perea, E. E. Mendez, and C. G. Fonstad, Appl. Phys. Lett. **36**, 978 (1980).
[33]P. M. Laufer, F. H. Pollak, R. E. Nahory, and M. A. Pollack, Solid State Commun. **36**, 419 (1980).
[34]J. A. Lahtinen and T. Tuomi, Phys. Status Solidi B **130**, 637 (1985).
[35]J. A. Lahtinen, Phys. Rev. B **33**, 2550 (1986).
[36]C. V. de Alvarez, J. P. Walter, M. L. Cohen, J. Stokes, and Y. R. Shen, Phys. Rev. B **6**, 1412 (1972).
[37]M. Welkowsky and R. Braunstein, Phys. Rev. B **5**, 497 (1972).
[38]P. Rochon and E. Fortin, Phys. Rev. B **12**, 5803 (1975).
[39]S. Gopalan, P. Lautenschlager, and M. Cardona, Phys. Rev. B **35**, 5577 (1987), and references therein.
[40]D. E. Aspnes, Opt. Commun. **8**, 222 (1973); D. E. Aspnes and A. A. Studna, App. Opt. **14**, 220 (1975); D. E. Aspnes and A. A. Studna, Rev. Sci. Instrum. **49**, 291 (1978).
[41]R. M. Azzam and N. N. Bashara, *Ellipsometry and Polarized Light* (North-Holland, Amsterdam, 1977).
[42]D. E. Aspnes, G. P. Schwartz, G. J. Gualtieri, A. A. Studna, and B. Schwartz, J. Electrochem. Soc. **128**, 590 (1981); It has come to our attention that optical data for the oxide on InP are also available: H. J. Lewerenz, D. E. Aspnes, B. Miller, D. L. Malm, and A. Heller, J. Am. Chem. Soc. **104**, 3325 (1982). The value of $\epsilon_1=2.2$ is somewhat smaller than that used here ($\epsilon_1=3.2$). This difference is compensated here by the use of a different oxide thickness so that, as shown in Fig. 2, no significant errors occur.
[43]A. Savitzky and M. J. E. Golay, Anal. Chem. **36**, 1627 (1964); corrections in J. Steinier, Y. Termonia, and J. Deltour, *ibid.* **44**, 1906 (1972).
[44]Y. Toyozawa, M. Inoue, T. Inui, M. Okazaki, and E. Hanamura, J. Phys. Soc. Jpn. Suppl. **21**, 133 (1966); **22**, 1337 (1967).
[45]J. E. Rowe and D. E. Aspnes, Phys. Rev. Lett. **25**, 162 (1970).
[46]P. Lautenschlager, P. B. Allen, and M. Cardona, Phys. Rev. B **33**, 5501 (1986).
[47]D. E. Aspnes, J. Opt. Soc. Am. **64**, 639 (1974).
[48]B. Velicky and J. Sak, Phys. Status Solidi **16**, 147 (1966).
[49]R. M. Martin, J. A. Van Vechten, J. E. Rowe, and D. E. Aspnes, Phys. Rev. B **6**, 2500 (1972).
[50]M. Cardona, in *Atomic Structure and Properties of Solids* (Academic, New York, 1972), p. 512.
[51]M. Cardona, in *Light Scattering in Solids II,* edited by M. Cardona and G. Güntherodt (Springer-Verlag, Berlin, 1982), p. 19.
[52]M. Cardona, Phys. Rev. B **15**, 5999 (1977).
[53]A. Daunois and D. E. Aspnes, Phys. Rev. B **18**, 1824 (1978).
[54]D. E. Aspnes and M. Cardona, Solid State Commun. **27**, 397 (1978).
[55]D. J. Chadi, Phys. Rev. B **16**, 790 (1977).